The Journal of Engine Research

Journal Homepage: www.engineresearch.ir

Thermal analysis of functionally graded materials in cylinders and pistons based on super element method

R. Pourhamid[1*], H. Mahdavy Moghaddam[2], A. Mohammadzadeh[3]

[1]*Department of Mechanics, Science and Research Branch, Islamic Azad University, Tehran, Iran, reza_pourhamid@yahoo.com*
[2]*Department of Mechanics, Science and Research Branch, Islamic Azad University, Tehran, Iran, mahdavy@srbiau.ac.ir*
[3]*Department of Mechanics, Science and Research Branch, Islamic Azad University, Tehran, Iran, dabir@srbiau.ac.ir*
[*]*Corresponding Author, Phone Number: +98-912-304-8981*

ARTICLE INFO

Article history:
Received: 24 October 2013
Accepted: 24 December 2013

Keywords:
Thermal analysis
Functionally graded material
Cylinder
Piston
Super element

ABSTRACT

In the present article, the thermal analysis of the cylinder and the piston in four-cylinder engines, made of functionally graded materials (FGMs), has been performed by using the super element method. The objective of using FGMs in the cylinder and the piston is to increase their performance. FGMs include a combination of ceramics and metals. Inside the cylinder, the ceramic is considered and outside the cylinder, there is the metal. On the top area of the piston, it is consumed that there is the ceramic and on the bottom, there is the metal. This combination causes a better wear property (according to proper wear characteristics of the ceramic) and also makes a thermal barrier system (according to low heat transfer properties of the ceramic). The wear benefit is inside the cylinder and the thermal barrier benefit is on the top area of the piston. Obtained results indicate that there is a good agreement between finite element and super elements methods. However, the number of super elements is so lower than the number of finite elements with the same accuracy in results. In addition, the power value, which is related to material properties of FGMs, has no significant effect on the temperature distribution and the temperature gradient.

1) Introduction

Recent researches on new applicable materials known as functionally graded materials (FGMs) illustrate that these materials have a good capability for resisting high temperatures and also severe temperature gradients. Nowadays, the application of FGMs can be an inventive phenomenon in internal combustion engines [1] and the FGM has not been used in the industry of internal combustion engines, until now. However, if we consider the thermal barrier coating system as a type of FGMs, they were used in Cummins engines, commercially.

Cylinders and pistons in internal combustion engines are such components that are exposed to high temperatures and severe temperature gradients. Low thermal conductivity and low coefficient of the thermal expansion have enabled FGMs to withstand higher temperature gradients for a given heat flux [2-4].

FGMs are a combination of different materials, including metals and ceramics. They are non-homogeneous on a microscopic scale and completely different from composites materials due to their continuously changing microscopic properties. The composition, which is varied from a ceramic-rich surface to a metal-rich surface according to a desired variation of the volume fraction of the two materials between two surfaces, can easily be manufactured. Usually, these changes are related to material parameters and they are considered as power or exponential functions in the radius or thickness directions of components [2, 5].

FGMs have two benefits according to its ceramic side. One benefit is proper wear properties and the other benefit is to make a thermal barrier system. Thermal barrier systems, applied to the combustion chamber and the piston of engines, cause higher combustion temperatures, increasing the thermal efficiency, or to achieve lower base metal temperatures. Both can cause an increase in fatigue life of high temperature components and also reduction in fuel consumption and some emissions such as hydrocarbons [6].

Among various FG structures, cylindrical components have been in an especial interest. The transient heat transfer analysis is a vital stage in developments of strength investigations such as the dynamic thermal buckling, the fatigue lifetime assessment under cyclic thermal loads, dynamic crack propagation and etc. Thus, scientists have performed several researches on FG cylinders by using finite element methods (FEMs). As an example, the nonlinear transient heat transfer of a thick-walled FG cylinder with temperature dependent material properties was investigated by Azadi and Shariyat [3]. They studied influences of various boundary conditions and different geometric parameters on the temperature distribution for various volume fractions.

Azadi and Azadi [4] investigated nonlinear transient heat transfer and thermo-elastic stress analyses of a thick-walled FG cylinder with temperature dependent materials and by using the Hermitian transfinite element method. They indicated that the temperature dependency effect is significant on both stress and temperature distributions.

The majority of well-known heat transfer analyses, performed so far for thick FG cylinders are generally restricted to uniform heating [7] or the steady state heat transfer [8-18] investigations. In these mentioned researches, semi-analytical and numerical approaches have been used to solve the problem. One of these numerical approaches is the finite element method (FEM). Investigating the thermal analysis of FG cylinders and FG pistons in the application of FGMs in internal combustion engines is so rare. Akhlaghi et al. [19] studied the heat loss and thermal stresses in direct injection diesel engines, using FGMs. They used a combination of finite element and finite difference methods.

Besides this time-consuming method with high calculations, a new approach, entitles the super element method (SEM), was developed by Ahmadian and Zangeneh [20]. They used super elements to perform the free vibration analysis of laminated stiffened plates. This approach was used for another case study of the structural analysis of laminated hollow cylinders by Ahmidian and Bonakdar [21]. Taghvaeipour et al. [22] presented an application of a new cylindrical element formulation in finite element structural analysis of FGM hollow cylinders. They illustrated that the SEM had a high accuracy and its results were in a good agreement with previous studies and also the conventional FEM in the modal analysis.

According to the literature review, two novelty of this research is to use the new approach, which is super elements, and apply this approach to real engine components.

In this article, the SEM is applied for the first time to analyze the thermal behavior of FG cylinders and FG pistons. FGMs vary through the thickness of the cylinder and through the longitudinal direction of the piston. Obtained results are compared to results of the FEM (by the ABAQUS software) for metal-rich and ceramic-rich materials. Then, varying the material properties based on the power law is investigated for the temperature distribution in figures for FG cylinders and FG pistons.

2) Governing equations

2-1) Material types

In this article, it is assumed that the outer side of the cylinder, there is a metal and in the inner side, there is a ceramic. For the piston, a ceramic is considered on the top area and a metal is assumed on the bottom area. The schematic view of these assumptions is illustrated in Figure 1.

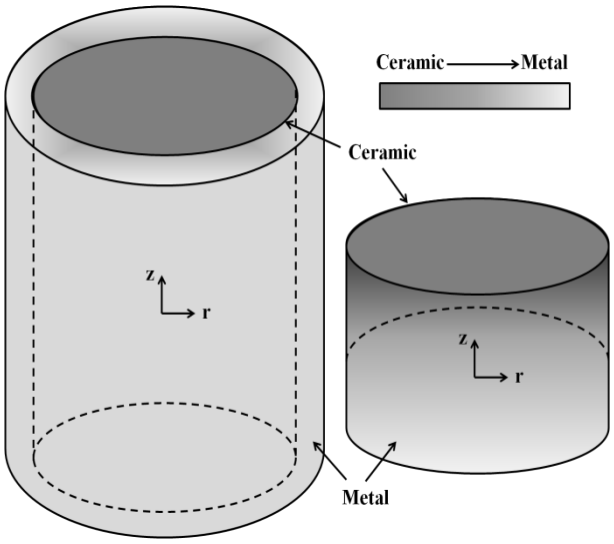

Figure 1: The schematic view of material distributions in the cylinder and the piston

The volume fraction for the cylinder is considered as a power low through its thickness.

$$V_m(r) = \left(\frac{r - r_i}{r_o - r_i}\right)^n \quad , \quad V_c(r) = 1 - V_m(r) \tag{1}$$

Where V_m and V_c is metal and ceramic volume fractions, respectively. Besides, r_i and r_o are internal and external radiuses of the cylinder, respectively. Also, n is a material constants.
Then, each material property (P) for the cylinder can be written as following,

$$P(T, r) = P_m(T)V_m(r) + P_c(T)V_c(r) \tag{2}$$

In which, P_m and P_c are metal and ceramic properties respectively.
The volume fraction for the piston is also considered as a power low through its length.

$$V_c(z) = \left(\frac{2z - L}{2L}\right)^n \quad , \quad V_m(z) = 1 - V_c(z) \tag{3}$$

Where L is the length of the cylinder. Then, each material property (P) for the piston can be written as following,

$$P(T, z) = P_m(T)V_m(z) + P_c(T)V_c(z) \tag{4}$$

In this research, the temperature dependency of material properties is not considered.

2-2) Shape functions

A super element is shown in Figure 2, which has 16 nodes. In this figure, r, α and z are radial, tangential and axial coordinates, respectively.
The relation between global (r, α, z) and local (η, γ, ξ) coordinates can be written as Equation (5).

$$\eta = \frac{2r - (r_i + r_o)}{r_o - r_i} \tag{5}$$

$$\gamma = \frac{\alpha}{\pi} - 1 \tag{6}$$

$$\xi = \frac{2z}{L} \tag{7}$$

For super elements, 16 shape functions (for each node) can be considered as a function of local variables as following,

$$N_i(\xi, \eta, \gamma) = \tilde{f}_i(\eta, \gamma, \xi) \tag{8}$$

These 16 shape functions are mentioned in the appendix. The sort type of super elements in the piston and the cylinder is shown in Figure 3. This sort type of super elements is selected according to the type of material distributions.

2-3) Governing equations

For the heat transfer in cylindrical coordinates, the main relation is as following,

$$\frac{1}{r}\frac{\partial}{\partial r}\left(kr\frac{\partial T}{\partial r}\right) + \frac{\partial}{\partial z}\left(k\frac{\partial T}{\partial z}\right) = \rho c_p \frac{\partial T}{\partial t} \tag{9}$$

Where T is the temperature, k is the thermal conductivity, ρ is the mass density and c_p is the specific heat. It should be mentioned that the $\partial/\partial\alpha$ term is not considered according to the axisymmetric problem.
Based on the Galerkin's method, or the residual integral function (R), the governing equation can be extracted by the following equation,

$$\int_v [N]^T R dv = 0 \quad : \quad dv = r dr d\alpha dz \tag{10}$$

$$R = \frac{1}{r}\frac{\partial}{\partial r}\left(kr\frac{\partial T}{\partial r}\right) + \frac{\partial}{\partial z}\left(k\frac{\partial T}{\partial z}\right) - \rho c_p \frac{\partial T}{\partial t} \tag{11}$$

In above equation, the temperature can be written based on the Kantorovich's approximation,

$$\{T(\eta, \gamma, \xi, t)\} = [N(\eta, \gamma, \xi)]_{1\times 16}\{T^{(e)}(t)\}_{16\times 1} \tag{12}$$

$$[N(\eta, \gamma, \xi)]_{1\times 16} = [N_1 \dots N_{16}] \tag{13}$$

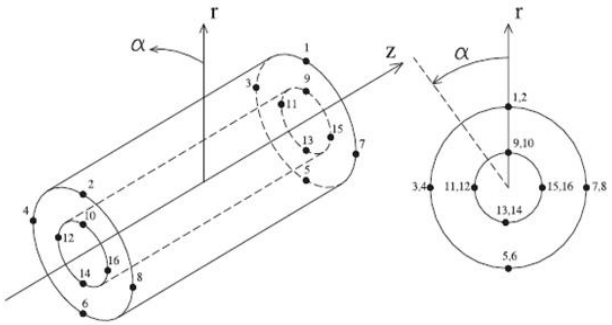

Figure 2: The super element with 16 nodes [22]

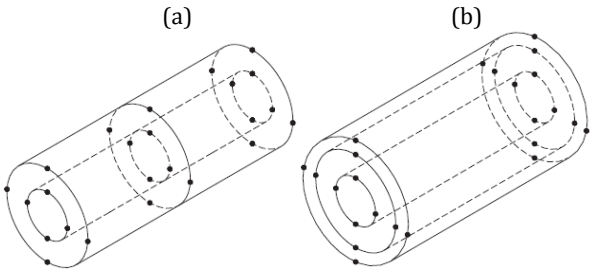

Figure 3: The sort type of super elements in (a) the piston and (b) the cylinder

Then, the governing equation can be simplified as following,

$$\left[C^{(e)}\right]\left\{\dot{T}^{(e)}(t)\right\}+\left[K^{(e)}\right]\left\{T^{(e)}(t)\right\}=\left\{f^{(e)}\right\} \tag{14}$$

$$\left[C^{(e)}\right]=-\int_{v}\rho c_p[N]^T[N]dv \tag{15}$$

$$\left[K^{(e)}\right]=\int_{v}[N]^T\left[\frac{1}{r}\frac{\partial}{\partial r}\left(kr\frac{\partial[N]}{\partial r}\right)+\frac{\partial}{\partial z}\left(k\frac{\partial[N]}{\partial z}\right)\right]dv \tag{16}$$

$$\left\{f^{(e)}\right\}=0 \tag{17}$$

By using the integration by part and the Gauss-Green's theory, $K^{(e)}$ can be rewritten as following,

$$\begin{aligned}\left[K^{(e)}\right]=&\int_{v}[N]^T\left[k_{,r}[N]_{,r}+\frac{k}{r}[N]_{,r}+k_{,z}[N]_{,z}\right]dv\\&+\int_{s}k[N]^T[N]_{,r}n_r ds\\&-\int_{v}\left(k_{,r}[N]^T+k[N]_{,r}^T\right)[N]_{,r}dv\\&+\int_{s}k[N]^T[N]_{,z}n_z ds\\&-\int_{v}\left(k_{,z}[N]^T+k[N]_{,z}^T\right)[N]_{,z}dv\end{aligned} \tag{18}$$

For the cylinder, the inner side is exposed to the heat flux due to the engine combustion. The outer side of the cylinder is exposed to the coolant (the water jacket). Therefore, these boundary conditions for the cylinder can be represented as following,

$$\begin{aligned}-k\frac{\partial T}{\partial r}&=q_0 \quad : \quad r=r_i\\-k\frac{\partial T}{\partial r}&=h(T-T_\infty) \quad : \quad r=r_o\end{aligned} \tag{19}$$

Where q_0, h, T_∞ are the heat flux due to the engine combustion, the coefficient of the convection heat transfer and the initial temperature, respectively.
Based on boundary conditions for the cylinder, the $K^{(e)}$ matrix and the $f^{(e)}$ vector can be rewritten as Equations (20) and (21).

$$\begin{aligned}\left[K^{(e)}\right]=&\int_{v}[N]^T\left[k_{,r}[N]_{,r}+\frac{k}{r}[N]_{,r}\right]dv\\&-\int_{r=r_o}h[N]^T[N]ds\\&-\int_{v}\left(k_{,r}[N]^T+k[N]_{,r}^T\right)[N]_{,r}dv\\&-\int_{v}k[N]_{,z}^T[N]_{,z}dv\end{aligned} \tag{20}$$

$$\left\{f^{(e)}\right\}=\int_{r=r_i}q_0[N]^T ds-\int_{r=r_o}hT_\infty[N]^T ds \tag{21}$$

It should be mentioned that in the cylinder the $\partial k/\partial z$ term is not considered. The reason is that the material properties change through the thickness and are constant through the longitudinal direction of the cylinder.
For the piston, the top area is exposed to the heat flux due to the engine combustion. Its bottom area is exposed to the coolant (the piston cooling jet). Therefore, these boundary conditions for the piston can be represented as following,

$$\begin{aligned}-k\frac{\partial T}{\partial z}&=q_0 \quad at \quad z=L/2\\-k\frac{\partial T}{\partial z}&=h(T-T_\infty) \quad at \quad z=-L/2\end{aligned} \tag{22}$$

In the piston, r_i is equal to zero.
Based on boundary conditions for the piston, the $K^{(e)}$ matrix and the $f^{(e)}$ vector can be rewritten as following,

$$\begin{aligned}\left[K^{(e)}\right]=&\int_{v}[N]^T\left[\frac{k}{r}[N]_{,r}+k_{,z}[N]_{,z}\right]dv\\&-\int_{v}k[N]_{,r}^T[N]_{,r}dv\\&-\int_{z=-L/2}h[N]^T[N]ds\\&-\int_{v}\left(k_{,z}[N]^T+k[N]_{,z}^T\right)[N]_{,z}dv\end{aligned} \tag{23}$$

$$\left\{f^{(e)}\right\}=\int_{z=L/2}q_0[N]^T ds-\int_{z=-L/2}hT_\infty[N]^T ds \tag{24}$$

It should be mentioned that in the cylinder the $\partial k/\partial r$ term is not considered. The reason is that material properties change through the longitudinal direction of the piston and not through its radius. In other word, material properties are constant through the radius of the piston.

2-4) Code inputs

A code is written in the MATLAB software (by using the ODE tool) to solve the governing equation. It should be mentioned that in this research, the radius of the piston is 71 mm, the inner radius of the cylinder is 71 mm and its outer radius is 81 mm, based on geometries in the four-cylinder engine. The length of the cylinder is 83.6 mm and the length of the piston is 27.9 mm.

The heat flux of the engine combustion can be estimated in following sentences. If the fuel consumption of the four-cylinder engine is considered as 8 lit per 100 km, for the speed of 90 km/h and 29.8 MJ/lit of the gasoline energy, the engine combustion makes 59600 J/s of the energy. This value of the heat flux is equal to 3763.4 kW/m^2 on the piston area at 3000 rpm of the engine speed. This heat flux will be produced in less than 0.02 s through the combustion step. The thermal analysis is performed at this time duration, while the initial temperature is considered as 300°C. The range of the heat flux value in the four-cylinder engine can be compared to another engine (the Peugeot engine), reported in the literature [23]. The range of the heat flux was reported about 4 to 5 MW/m^2 [23] on the piston area, in less than 0.02 s of the combustion duration, at 2500 rpm (Figure 4).

Besides, the value of h is assumed to be 5000 W°C/m^2 for both coolants. The range of this value, which is considered for the four-cylinder engine, can be compared with another four-cylinder engine, reported in the literature [23]. For the water coolant, the averaged value for h was reported as an averaged value of 5000 W°C/m^2 [24].

For this thermal analysis, material properties of studied FGMs are presented in Table 1. The metal is considered as Ti-6Al-4V and the ceramic is assumed to be Si_3N_4. The titanium alloy can be used in engine components as an inventive material due to its high ratio of the strength to the weight.

3) Finite element modeling

The material behavior of FGMs cannot be simulated in finite element commercial softwares such as ANSYS and ABAQUS codes. The reason is the power law for material modeling of FGMs, which cannot be applied to numerical softwares. In some cases, FGMs are modeled as a multi-layered material which assumption is not correct due to the discontinuity of material properties. Therefore, usually a code based on finite element methods (FEMs) should be written for solving governing equations in FGMs. In this research, to validate results obtained by the SEM, the cylinder and piston are modeled in the ABAQUS software, when they are considered as metal-rich and ceramic-rich materials, separately. Then, results of the SEM and the FEM are compared together for the validation.

For the FEM, axisymmetric models for the cylinder and the piston are considered in the ABAQUS software. Meshed models are shown in Figure 5. For these models, the convergency of results is checked and then, 2100 finite elements (2210 nodes) and 7952 finite elements (8136 nodes) are considered for the cylinder and the piston, respectively.

4) Results and discussions

4-1) Validation process

In this part, the case study in this research can be validated by experimental data of another engine. This is due to the unavailability of experimental data for the four-cylinder engine. Also, there are some limitations for this validation. Only results of a temperature survey test of the cylinder can be found on the other four-cylinder engine, reported in the literature [25]. Besides these limitations, a simple geometry (and not a real geometry) is considered for FE modeling of the cylinder. Thus, in this part, we want to show that obtained results are in a proper range, in comparison to experimental data. Besides, it is indicated that the thermal analysis process can be verified by experimental temperatures.

The inner radius and the outer radius of the cylinder in the other four-cylinder engine is 78.6 and 88.6 mm. Also, its length is 85.0 mm. The initial temperature is considered as 200°C. Other parameters are the same as the case study in this research. The material of the cylinder in the other four-cylinder engine is EN-GJL-250 cast iron [24]. The thermal conductivity, the mass density and the specific heat are considered as 46.5 W/m.K, 7200 kg/m^3 and 460 J/kg.K, respectively.

Table 1: Material properties for the studied FGM [3-4]

Characteristics	Metal (Ti-6Al-4V)	Ceramic (Si_3N_4)
$\rho\ \left(\frac{kg}{m^3}\right)$	2370	4429
$c_p\ \left(\frac{J}{kg.K}\right)$	625.30	555.11
$k\ \left(\frac{W}{m.K}\right)$	13.72	1.21

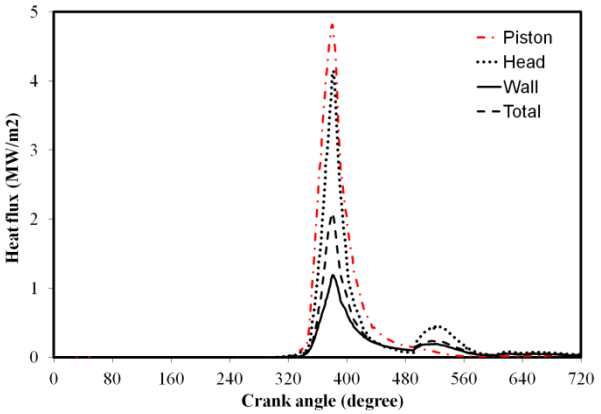

Figure 4: The heat flux on the piston, the head and the wall of the combustion chamber and the total heat flux [23]

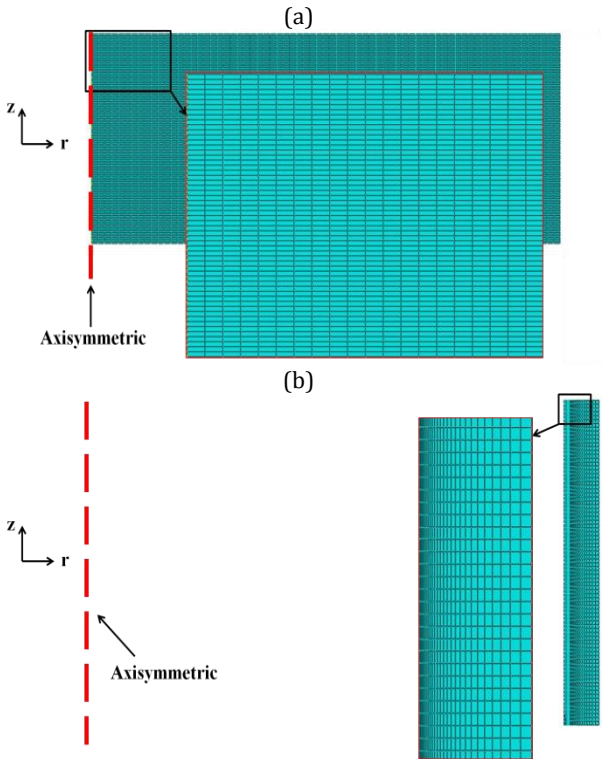

Figure 5: A part of FE models of (a) the piston and (b) the cylinder in the ABAQUS software

Results of the temperature distribution in the full FE model of the cylinder are shown in Figure 6(a). The related FE analysis was performed in the literature [25]. Then, it was compared to experimental data, obtained from a temperature survey test, which was performed on an engine test bed. In this test, thermocouples were installed below the bridge of cylinders. The temperature was measured during engine working at 4000 rpm and full-loaded conditions. Measured temperatures are constant during a steady state condition. It means that at each point of testing, a time duration is considered. Then, the temperature will become steady at that time duration [25]. The maximum temperature, measured in the temperature survey test, is about 240°C on the bridge. Besides, by the full FE model of the cylinder, the maximum temperature was obtained about 235°C [25], which is so near to experimental data. In Figure 6(b), results of the simple FE model (including only a cylinder) are shown.

By using the simple FE model of the cylinder in Figure 6(b), the maximum temperature is calculated about 248°C, which shows the verification of the FE process. This temperature is higher than that value in the full FE model. As this simple FE model is for only one cylinder, the area of the heat transfer is lower and therefore, the temperature is predicted higher.

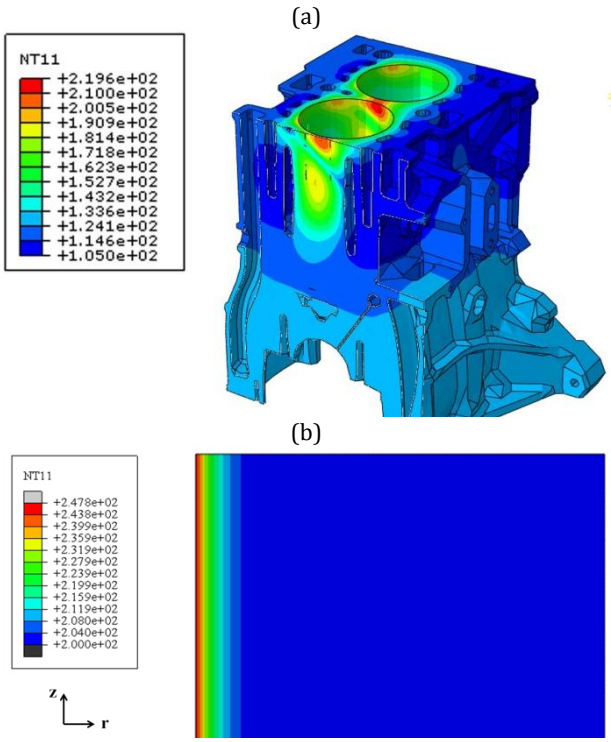

Figure 6: The comparison of numerical and experimental results for the cylinder of the other four-cylinder engine, including (a) results reported in the literature [25] and (b) results of the simple FE model with a simple geometry of the cylinder

4-2) FG cylinder

As the first result, the number of super elements should be considered to investigate the convergency of the numerical approach. The temperature distribution of the metal-rich (n=0) cylinder is drawn in Figure 7. By increasing the number of super elements, the temperature gradient increases. Based on these results for the cylinder in this figure, 20 super elements (with 168 nodes) are considered for obtaining all other results, where the temperature gradient changes so little in comparison to 25 super elements. Besides, in comparison to 2100 finite elements (2210 nodes) used in the ABAQUS software for the cylinder, this number of super elements shows the same accuracy and lower time of calculations.

The distribution of volume fractions (for the metal and the ceramic) is shown in Figure 8 versus the radius of the cylinder. In this figure, volume fractions are drawn for various values of n, the power in Equation (21). It should be mentioned that when n is zero, the FGM becomes exactly a metal-rich material. Also, considering 30 for n is approximately equal to the ceramic-rich material. In this condition, less than 10% of the material is metal. As another note, it should be mentioned that for n=1, the material behavior becomes linear.

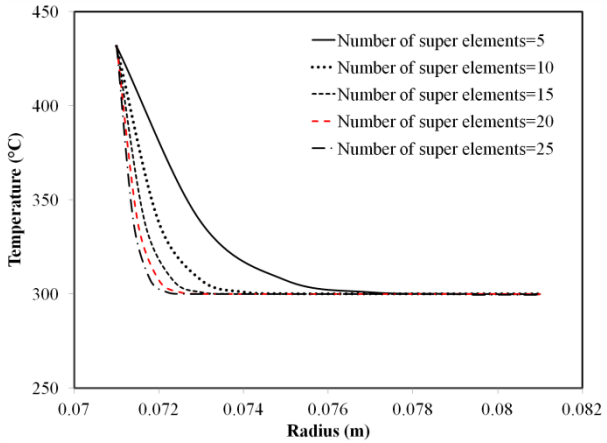

Figure 7: The temperature distribution in the metal-rich cylinder for different numbers of elements

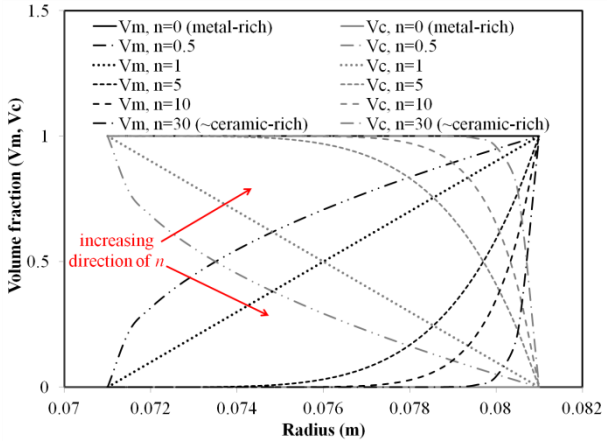

Figure 8: The distribution of volume fractions versus the radius of the cylinder for various values of *n*

Before mentioning main results, the validation of results, obtained by the SEM, should be presented. This is done in Figure 9. The maximum temperature is about 432°C and 623°C for metal-rich and ceramic-rich materials in the cylinder. In comparison to the metal-rich material, the error between these two methods becomes higher in the ceramic-rich material, where the temperature gradient is higher. The reason is due to the thermal conductivity. This property of the ceramic is about 10 times lower than that value of the metal. Since this transient behavior has a higher rate in the ceramic, the SEM with 40 super elements has lower accuracy to predict the temperature, in comparison to the FEM. This problem will be solved by considering higher number of super elements. In this condition, likewise, the number of super elements is so lower than the number of finite elements. However, as shown in Figure 9, a proper agreement can be observed between two methods and the error of the SEM can be neglectable. Besides, the number of super elements is so lower than the number of finite elements with the same accuracy.

The temperature distribution in a half body of the cylinder head is shown in Figure 10, when a metal-rich material is considered in the ABAQUS software. This result is related to the thermal analysis after 0.02 s of the combustion step. The maximum temperature is about 432°C for the metal-rich FGM in the cylinder, while the initial temperature is 300°C. This maximum temperature exists in the first layers of the FGM at the inner radius of the cylinder. Since the time of the combustion is so low (less than 0.02 s) and therefore, a high temperature gradient occurs.

The temperature distribution for different values of *n* can be observed in Figure 10. The maximum temperature is the same for all values of *n* due to have a ceramic-rich material in the outer radius of the cylinder (Figure 8). Obtained results in this figure show that the effect of the material distribution is not significant on the thermal behavior, when *n* changes from 1 to 10. There is only a small difference for the results of *n*=0.5 to other values. In this case, a higher volume of the material is metallic (Figure 8).

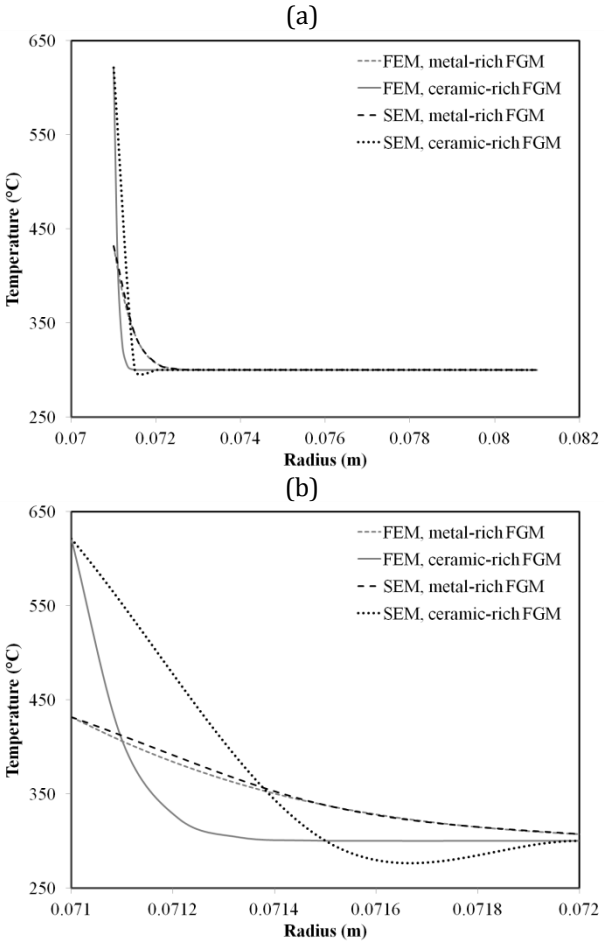

Figure 9: The comparison between FEM and SEM results for the cylinder made of metal-rich and ceramic-rich materials; (a) through the whole radius and (b) by higher magnification (near the internal radius of the cylinder)

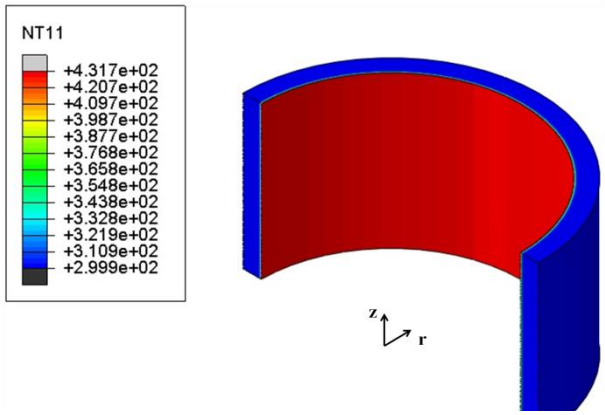

Figure 10: The temperature distribution for the metal-rich cylinder, obtained by the ABAQUS software

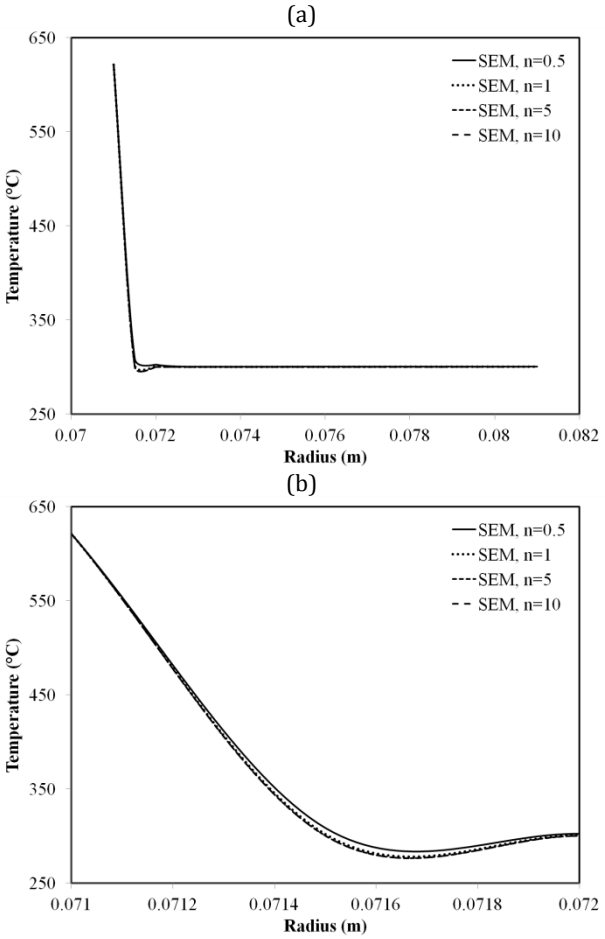

Figure 11: The temperature distribution in the FG cylinder for different values of *n* by using the SEM; (a) through the whole radius and (b) by higher magnification (near the internal radius of the cylinder)

4-3) FG piston

Figure 12 indicates the temperature distribution of the metal-rich piston. By increasing the number of super elements, the temperature gradient increases through the length of the piston.

Based on these results for the piston in this figure, 40 super elements (with 328 nodes) are considered for obtaining all other results, where the temperature gradient changes so little in comparison to that one by using 45 super elements. Besides, in comparison to 7952 finite elements (8136 nodes) used in the ABAQUS software for the piston, this number of super elements shows the same accuracy and lower time of calculations. Figure 13 indicates the distribution of volume fractions (for the metal and the ceramic) versus the length of the piston. In this figure, volume fractions are drawn for various values of *n*, the power in Equation (23). It should be mentioned that when *n* is zero, the FGM becomes exactly a ceramic-rich material. Also, considering 30 for *n* is approximately equal to the metal-rich material. In this condition, less than 10% of the material includes the ceramic material.

The validation of results, obtained by the SEM, is presented in Figure 14. The maximum temperature is about 430°C and 512°C for metal-rich and ceramic-rich materials in the piston. These temperatures are lower than those ones in the cylinder. Since, the heat transfer area in the piston is more than the area in the cylinder.

In comparison to the metal-rich material, the error between these two methods becomes higher in the ceramic-rich material, where the temperature gradient is also higher.

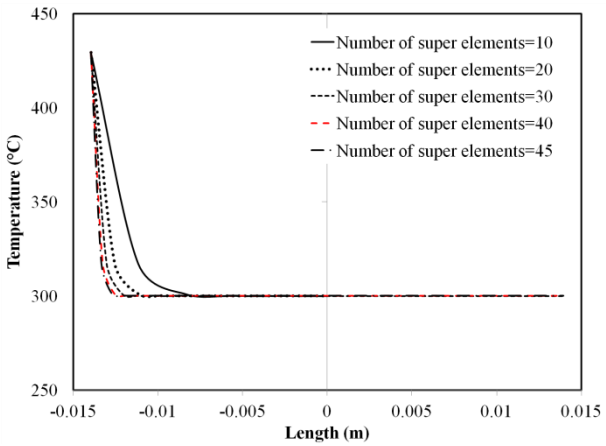

Figure 12: The temperature distribution in the metal-rich piston for different numbers of elements

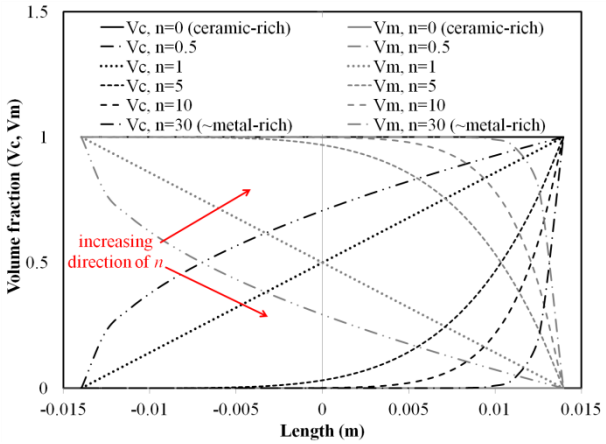

Figure 13: The distribution of volume fractions versus the length of the piston for various values of *n*

As mentioned for the FG cylinder, the transient behavior in the ceramic is higher than that one in the metal due to their thermal conductivity. Higher number of super elements can be used to increase the accuracy. As demonstrated in Figure 14, a good agreement can be observed between results of two methods (the SEM and the FEM) and the error of results in the SEM can be neglectable. Besides, the number of super elements is so lower than the number of finite elements, although they have the same accuracy.

The temperature distribution in a half of the piston is indicated in Figure 15, when a metal-rich material is considered for the piston in the ABAQUS software. This result is related to the thermal analysis after 0.02 s of the combustion step. The maximum temperature reaches to about 430°C for the metal-rich FGM in the piston, while the initial temperature is assumed to be 300°C. This temperature is considered as a steady state temperature during the combustion.

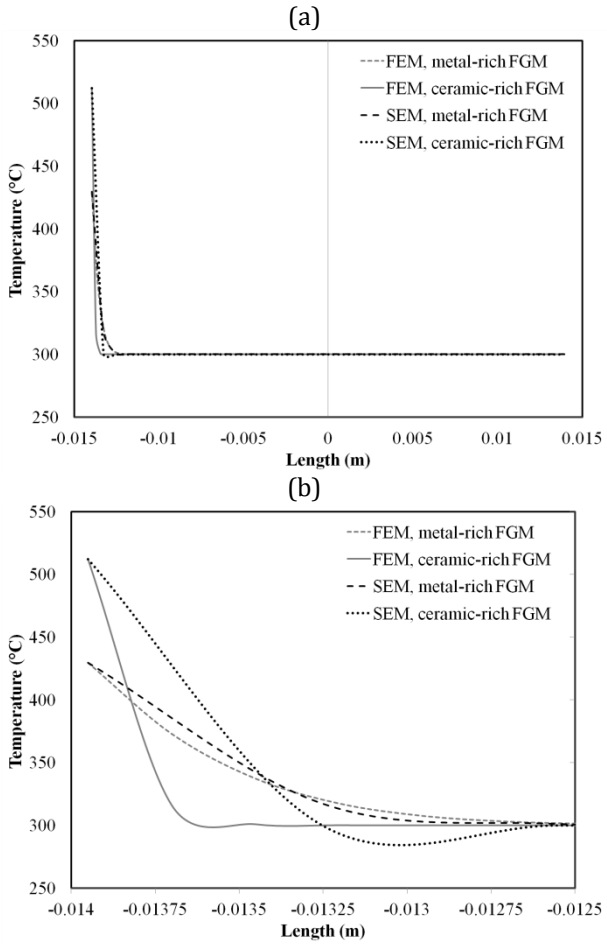

Figure 14: The comparison between FEM and SEM results for the piston made of metal-rich and ceramic-rich materials; (a) through the whole length and (b) by higher magnification (near the top area of the piston)

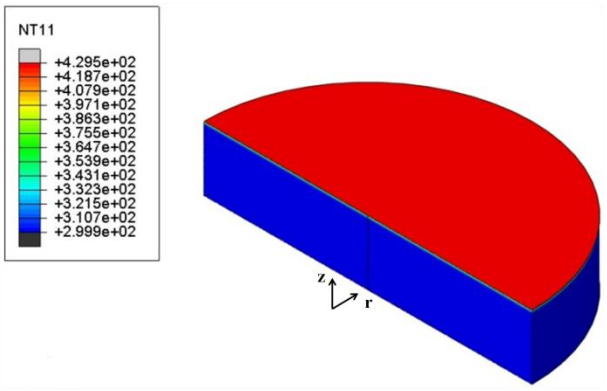

Figure 15: The temperature distribution for the metal-rich piston, obtained by the ABAQUS software

The temperature distribution for different values of *n* is demonstrated in Figure 16. The maximum temperature is the same for all values of *n* due to have a ceramic-rich material on the top area of the piston (as can be observed in Figure 13). Obtained results illustrate that the effect of the material distribution is not significant on the temperature distribution in the piston. The behavior is observed also for the cylinder. Thus, it can be said that there is no large effect on the temperature distribution and the temperature gradient by changing the material distribution in the cylinder or in the piston.

4-4) Optimization process

To optimize the material distribution, an optimum value for *n* should be obtained. Based on results by the SEM for different values of *n*, it can be said that if the maximum temperature is selected as an objective for the optimization, then a low value (such as 0.5 or also lower value) can be introduced as the optimum value. In other words, only a thin layer of the ceramic requires to have a thermal barrier and to obtain higher maximum temperature in comparison to the metal. Then, this type of the FGM will be similar to the thermal barrier coatings, but not in discontinuous properties. This higher temperature in the combustion chamber will lead to higher performance in engines. The ceramic layer should be placed in the inner radius of the cylinder and also should be placed on the top area of the piston, where are exposed to the heat flux of the combustion.

In addition, only the maximum temperature is not a proper objective for the optimization of the material distribution in FGMs. Some other parameters should be added to target functions for a better optimization. Besides the maximum temperature, these parameters can be introduced as the thermal stress, the weight and costs of manufacturing of FGMs. Considering all these parameters will lead to have a proper optimization process. This work will be appeared in next researches, in the future.

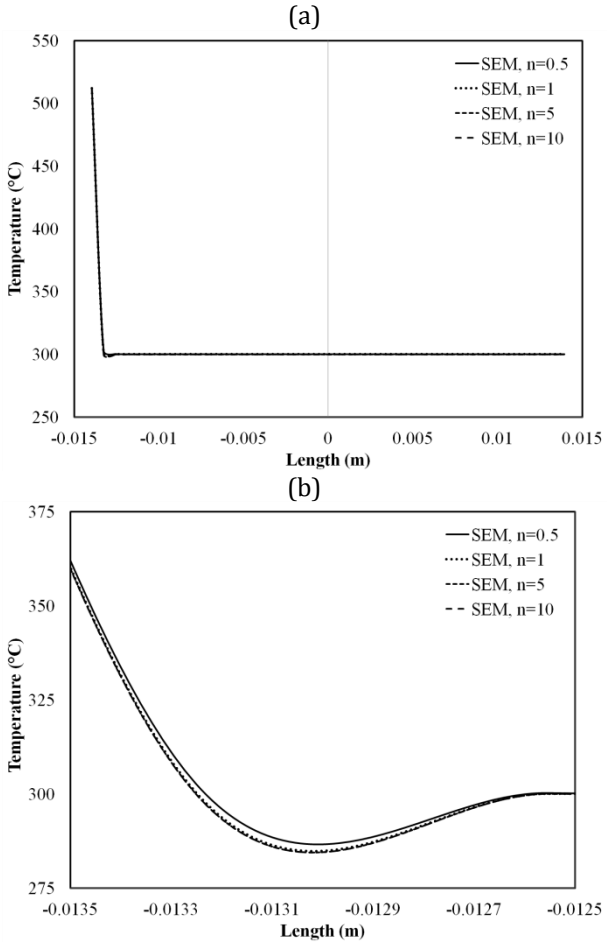

Figure 16: The temperature distribution in the FG piston for different values of *n* by using the SEM; (a) through the whole length and (b) by higher magnification (near the top area of the piston)

5) Conclusion

In this research, the thermal analysis of FG cylinders and FG pistons in engines is presented by using the SEM. Super elements include shallow cylindrical elements with 8 nodes in each element, which can be used in cylinders and pistons. Obtained results show that the accuracy of the SEM is the same as the FEM, although the number of super elements is so lower than the number of finite elements. Therefore, the time of calculations is also so lower in the SEM, in comparison to the FEM. In other words, the SEM offers a relatively simple and efficient means of predicting the material behavior with much shorter runtime.

In addition, obtained results by the SEM indicate that there is no significant effect in changing of *n* (in the power law for FGM behavior modeling) on the temperature distribution and the temperature gradient. The behavior occurs in the cylinder and in the piston, made of FGMs.

Appendix

For super elements, 16 shape functions (for each node in one super element) can be written in the local coordinate as Equation (A1).

$$
\begin{aligned}
N_1(\xi,\eta,\gamma) &= \frac{1}{8}(cos^2\pi\gamma - cos\pi\gamma)(1+\xi)(1+\eta)\\
N_2(\xi,\eta,\gamma) &= \frac{1}{8}(cos^2\pi\gamma - cos\pi\gamma)(1-\xi)(1+\eta)\\
N_3(\xi,\eta,\gamma) &= \frac{1}{8}(sin^2\pi\gamma - sin\pi\gamma)(1+\xi)(1+\eta)\\
N_4(\xi,\eta,\gamma) &= \frac{1}{8}(sin^2\pi\gamma - sin\pi\gamma)(1-\xi)(1+\eta)\\
N_5(\xi,\eta,\gamma) &= \frac{1}{8}(cos^2\pi\gamma + cos\pi\gamma)(1+\xi)(1+\eta)\\
N_6(\xi,\eta,\gamma) &= \frac{1}{8}(cos^2\pi\gamma + cos\pi\gamma)(1-\xi)(1+\eta)\\
N_7(\xi,\eta,\gamma) &= \frac{1}{8}(sin^2\pi\gamma + sin\pi\gamma)(1+\xi)(1+\eta)\\
N_8(\xi,\eta,\gamma) &= \frac{1}{8}(sin^2\pi\gamma + sin\pi\gamma)(1-\xi)(1+\eta)\\
N_9(\xi,\eta,\gamma) &= \frac{1}{8}(cos^2\pi\gamma - cos\pi\gamma)(1+\xi)(1-\eta)\\
N_{10}(\xi,\eta,\gamma) &= \frac{1}{8}(cos^2\pi\gamma - cos\pi\gamma)(1-\xi)(1-\eta)\\
N_{11}(\xi,\eta,\gamma) &= \frac{1}{8}(sin^2\pi\gamma - sin\pi\gamma)(1+\xi)(1-\eta)\\
N_{12}(\xi,\eta,\gamma) &= \frac{1}{8}(sin^2\pi\gamma - sin\pi\gamma)(1-\xi)(1-\eta)\\
N_{13}(\xi,\eta,\gamma) &= \frac{1}{8}(cos^2\pi\gamma + cos\pi\gamma)(1+\xi)(1-\eta)\\
N_{14}(\xi,\eta,\gamma) &= \frac{1}{8}(cos^2\pi\gamma + cos\pi\gamma)(1-\xi)(1-\eta)\\
N_{15}(\xi,\eta,\gamma) &= \frac{1}{8}(sin^2\pi\gamma + sin\pi\gamma)(1+\xi)(1-\eta)\\
N_{16}(\xi,\eta,\gamma) &= \frac{1}{8}(sin^2\pi\gamma + sin\pi\gamma)(1-\xi)(1-\eta)
\end{aligned}
\qquad \text{(A1)}
$$

Acknowledgement

Authors would like to thank Irankhodro Powertrain Company (IPCO) and also Saipa Company for their supporting in experimental data of internal combustion engines. Besides, authors also thank Dr. M. Azadi for his helps.

References

[1] N. Sasaki, S. Nogawa, D. Takahashi, Engine cooling apparatus, Patent Application Number: 20120204820, 2012

[2] M. Damircheli, M. Azadi, Temperature and thickness effects on thermal and mechanical stresses of rotating FG-disks, Journal of Mechanical Science and Technology, Vol. 25, No. 3, pp. 1-9, 2011

[3] M. Azadi, M. Shariyat, Nonlinear transient transfinite element thermal analysis of thick-walled FGM cylinders with temperature-dependent material properties, Meccanica, Vol. 45, No. 3, pp. 305-318, 2010

[4] M. Azadi, M. Azadi, Nonlinear transient heat transfer and thermoelastic analysis of thick-walled FGM cylinder with temperature-dependent material properties using Hermitian transfinite element, Journal of Mechanical Science and Technology, Vol. 23, No. 10, pp. 2635-2644, 2009

[5] M. Azadi, Free and forced vibration analysis of FG-beam considering temperature dependency of material properties, Journal of Mechanical Science and Technology, Vol. 25, No. 1, pp. 69-80, 2011

[6] A. Moridi, M. Azadi, G.H. Farrahi, Thermo-mechanical stress analysis of thermal barrier coating system considering thickness and roughness effects, Surface and Coatings Technology, 2012, DOI: 10.1016/j.surfcoat.2012.02.019
[7] R.W. Zimmerman, M.P. Lutz, Thermal stress and thermal expansion in a uniformly heated functionally graded cylinder, Journal of Thermal Stress, Vol. 22, pp. 88-177, 1999
[8] Y. Obata, N. Noda, Steady thermal stresses in a hollow circular cylinder and a hollow sphere of a functionally gradient material, Journal of Thermal Stress, Vol. 17, pp. 471-487, 1994
[9] N. El-abbasi, S.A. Meguid, Finite element modeling of the thermoelastic behavior of functionally graded plates and shells, International Journal of Computational Engineering Science, Vol. 1, pp. 51-165, 2000
[10] M. Jabbari, S. Sohrabpour, M.R. Eslami, Mechanical and thermal stresses in a functionally graded hollow cylinder due to radially symmetric loads, International Journal of Pressure Vessels and Piping, Vol. 493, pp. 479-497, 2002
[11] K.M. Liew, S. Kitipornchai, X.Z. Zhang, C.W. Lim, Analysis of the thermal stress behavior of functionally graded hollow circular cylinders, International Journal of Solids Structures, Vol. 40, pp. 2355-2380, 2003
[12] M. Jabbari, S. Sohrabpour, M.R. Eslami, General solution for mechanical and thermal stresses in a functionally graded hollow cylinder due to nonaxisymmetric steady state loads, ASME Journal of Applied Mechanics, Vol. 70, pp. 111-118, 2003
[13] H.S. Shen, Thermal postbuckling behavior of functionally graded cylindrical shells with temperature dependent properties, International Journal of Solids Structures, Vol. 41, pp. 1961-1974, 2004
[14] Y. Ootao, Y. Tanigawa, Two-dimensional thermo-elastic analysis of a functionally graded cylindrical panel due to nonuniform heat supply, Mechanics Research Communications, Vol. 32, pp. 429-443, 2005
[15] S.M. Hosseini, M. Akhlaghi, M. Shakeri, Transient heat conduction in functionally graded thick hollow cylinders by analytical method, Heat and Mass Transfer, Vol. 43, pp. 669-675, 2007
[16] M.H. Babaei, Z.T. Chen, Hyperbolic heat conduction in a functionally graded hollow sphere, International Journal of Thermophysics, Vol. 29, pp. 1457-1469, 2008
[17] I. Keles, C. Conker, Transient hyperbolic heat conduction in thick-walled FGM cylinders and spheres with exponentially-varying properties, European Journal of Mechanics, A/Solids, Vol. 30, No. 3, pp. 449-455, 2011
[18] L. Cao, H. Wang, Q.H. Qin, Fundamental solution based graded element model for steady state heat transfer in FGM, Acta Mechanica Solida Sinica, Vol. 25, No. 4, pp. 377-392, 2012
[19] M. Akhlaghi, A. Zamani, S.M. Hosseini, Heat loss and thermal stresses in DI diesel engine using functionally graded cylinder (FGMs), Recent Advances in Composite Materials, 2007
[20] M.T. Ahmadian, M.S. Zahgeneh, Application of super elements to free vibration analysis of laminated stiffened plates, Journal of Sound and Vibration, Vol. 259, No. 5, pp. 1243-1252, 2003
[21] M.T. Ahmadian, M. Bonakdar, A new cylindrical element formulation and its application to structural analysis of laminated hollow cylinders, Finite Elements in Analysis and Design, Vol. 44, pp. 617-630, 2008
[22] A. Taghvaeipour, M. Bonakdar, M.T. Ahmadian, Application of a new cylindrical element formulation in finite element structural analysis of FGM hollow cylinders, Finite elements in Analysis and Design, Vol. 50, pp. 1-7, 2012
[23] A. Mohammadi, Heat transfer analysis on engine combustion chamber by using of KIVA code, Shiraz University, Shiraz, Iran, 2007
[24] R. Hemat Khanlou, Studying of boiling phenomenon in cooling passage of EF7TC and investigating the parameters effect, K.N. University of Technology, Tehran, Iran, 2012
[25] M. Azadi, General temperature survey of cylinder block and head, Technical Report, Irankhodro Powertrain Company (IPCO), Tehran, Iran, 2010

فصلنامهٔ علمی- پژوهشی تحقیقات موتور

تارنمای فصلنامه: www.engineresearch.ir

تحلیل حرارتی مواد هدفمند در استوانه‌ها و سمبه‌ها بر اساس روش اجزاء برتر

رضا پورحمید[۱*]، حسین مهدوی مقدم[۲]، علیرضا محمدزاده[۳]

[۱] گروه مکانیک، دانشگاه آزاد اسلامی، واحد علوم تحقیقات تهران، تهران، ایران، reza_pourhamid@yahoo.com
[۲] گروه مکانیک، دانشگاه آزاد اسلامی، واحد علوم تحقیقات تهران، تهران، ایران، mahdavy@srbiau.ac.ir
[۳] گروه مکانیک، دانشگاه آزاد اسلامی، واحد علوم تحقیقات تهران، تهران، ایران، dabir@srbiau.ac.ir
[*] نویسندهٔ مسئول، شمارهٔ تماس: ۰۹۱۲۲۷۷۵۷۹۸

چکیده

در این مقاله، تحلیل حرارتی استوانه و سمبه در موتورهای چهار استوانه‌ای، ساخته شده از مواد هدفمند، با استفاده از روش اجزاء برتر، انجام شده است. هدف از بکارگیری مواد هدفمند در استوانه و سمبه، افزایش عملکرد آنهاست. مواد هدفمند شامل ترکیبی از سفال‌ها و فلزات اند. در داخل استوانه، ماده از جنس سفال و در سطح خارجی آن، ماده از جنس فلز است. جنس روی تاج سمبه، سفال و سطح زیرین آن از فلز فرض شده است. این ترکیب باعث ایجاد خواص سایشی بهتر (بر اساس خواص سایشی سفال) می‌شود. همچنین، این ترکیب باعث ایجاد محافظ گرمایی (براساس خواص ضعیف انتقال حرارت سفال) می‌گردد. مزیت خواص سایشی برای سطح داخل استوانه و مزیت محافظ گرمایی برای سطح روی تاج سمبه مطرح است. نتایج تحلیل تطابق مناسبی بین روش‌های اجزاء محدود و اجزاء برتر را نشان می‌دهند. درحالی‌که تعداد اجزاء روش اجزاء برتر بسیار کمتر از تعداد اجزاء روش اجزاء محدود، با همان دقت نتایج است. همچنین، نتایج نشان می‌دهند که مقدار توان مربوط به خواص مواد هدفمند، تاثیر زیادی بر توزیع دما ندارد.

اطلاعات مقاله

تاریخچهٔ مقاله:
دریافت: ۰۲ آبان ۱۳۹۲
پذیرش: ۰۳ دی ۱۳۹۲

کلیدواژه‌ها:
تحلیل حرارتی
مواد هدفمند
استوانه
سمبه
اجزاء برتر